Supplement of Biogeosciences, 21, 2973–2994, 2024
https://doi.org/10.5194/bg-21-2973-2024-supplement

Supplement of

Integration of tree hydraulic processes and functional impairment to capture the drought resilience of a semiarid pine forest

Daniel Nadal-Sala et al.

Correspondence to: Rüdiger Grote (ruediger.grote@kit.edu)

Tables:

Table S1: LandscapeDNDC soil initialization for Yatir forest (Note that the current model setting disregards the wilting point as the soil moisture below which no water uptake is possible anymore. This point is replaced by the disconnection threshold water potential ($\Psi_{disconnect}$).)

Depth	clay content	field capacity	wilting point	soil organic content	bulk density	sceleton content	saturated water conductivity
(cm)	(%)	%	%	%	g cm^{-3}	%	cm min^{-1}
2-0	0	70	8	40	0.3	0	1.5.
0-5	30	30	8	3	1.65	0	0.09
5-15	30	30	8	2	1.57	5	0.09
15-25	40	27.5	8	2	1.61	10	0.10
25-35	42	27.5	9	1	1.54	20	0.11
35-50	42	27.5	11	1	1.54	20	0.11
50-100	42	28	11	1	1.54	30	0.11

Table S2: LandscapeDNDC parameters for *Pinus halepensis* regarding photosynthesis, phenology and allometry.

Description	unit	abbreviation	value	source
Photosynthesis				
activation energy for electron transport	J mol^{-1}	aejm	57550.0	Simioni et al. (2016)
activation energy for Michaelis-Menten constant for CO_2	J mol^{-1}	aekc	79430.0	Simioni et al. (2016)
activation energy for Michaelis-Menten constant for O_2	J mol^{-1}	aeko	36380.0	Simioni et al. (2016)
activation energy for dark respiration	J mol^{-1}	aerd	84450.0	Simioni et al. (2016)
activation energy for photosynthesis	J mol^{-1}	aevc	67390.0	Simioni et al. (2016)
relation between maximum electron transport rate and RubP saturated rate of carboxylation	--	qjvc	1.5	Maseyk et al. (2008a)
relation between dark respiration rate and RubP saturated rate of carboxylation at 25 °C	µmol m^{-2} s^{-1}	qrd25	0.011	Sperlich et al. (2015)
maximum stomata conductivity	mmolH_2O m^{-2} s^{-1}	gsmax	115.0	Baquedano and Castillo (2007)

deactivation energy (for electron transport processes)	J mol^{-1}	hdj	200000.0	Simioni et al. (2016)
entropy term of electron transport	J mol^{-1} °C^{-1}	sdj	685.0	calibrated *
maximum RubP saturated rate of carboxylation at 25 °C for sun leaves	µmol m^{-2} s^{-1}	vcmax25	38.8	Kuusk et al. (2018)
slope of foliage conductivity in response to assimilation in the BERRY-BALL model	--	slope_gsa	5.04	Maseyk et al. (2008a)
Phenology/ Turnover				
minimum temperature sum for foliage activity onset	°C	gddfolstart	0	Maseyk et al. (2008b)
total leaf longevity from the first day of the emergent year	days	dleafshed	1365	Maseyk et al. (2008b)
time interval necessary to complete growth of new foliage	days	ndflush	180	Maseyk et al. (2008b)
time interval necessary to complete litterfall of foliage	days	ndmorta	300	Maseyk et al. (2008b)
fraction of current fine root biomass that dies daily	--	tofrtbas	0.0005	Simioni et al. (2016)
fraction of current sapwood biomass that can die per day	--	tosapmax	0.00025	Cohen et al. (2008)
Allometry				
foliage biomass under optimal, closed canopy condition	kg m^{-2}	mfolopt	0.36	Maseyk et al. (2008b)
distribution parameter for foliage biomass	--	pfl	1.3	Zinsser (2017)
distribution parameter for fine root biomass	--	psl	0.91	Preisler et al. (2019)
ratio between fine root- and foliage biomass under standard conditions	--	qrf	0.41	Klein and Hoch (2015)
Minimum sapwood area to leaf area ratio (Huber value)	m^2 cm^{-2}	qsf	4.1	Froux et al. (2002)

***** calibrated for this study to the relation between observed photosynthesis and simulated temperature. This is preferred over using a standard value of 642 (Maseyk et al., 2008a) since the estimation of leaf temperature in LandscapeDNDC is subject to high uncertainty.

Table S3: Prior distribution implemented in the model inverse Bayesian calibration. Given are the mean and the standard deviation, as well as the upper and lower bounds for each parameter following a truncated gaussian distribution. *RPMIN* is the minimum whole-plant resistance to water flow; *ANSL* is the shape coefficient and ΨNSL is the reference $\Psi_{canopy,PD}$ coefficient of the drought impact function to assimilation; $\Psi_{disconnect}$ is the soil water potential at which roots do not re-equilibrate their water potential with soil water potential overnight; and *KSPEC* is the maximum root-to-canopy conductance per unit of leaf area.

Parameter	Mean	SD	Lower bound	Upper bound
RPMIN	4.5	0.5	1.5	8
ANSL	4	0.25	3	6
ΨNSL	-1.3	0.1	-2	-1
$\Psi_{disconnect}$	-2	0.3	-1.5	-2.5
KSPEC	1.5	0.3	0.5	3.0

Table S4: Simulated water balance at Yatir forest for the years of investigation.

Year	PREC [mm a-1]	TRANSP [mm a-1]	ECEP [mm a-1]	ESOIL [mm a-1]	PERC [mm a-1]	ΔSTORE [mm a-1]
2012	257	163	23	20	68	-18
2013	250	98	17	15	29	91
2014	183	177	27	35	23	-78
2015	247	165	31	32	25	-7
Average	234	151	25	25	36	-3
% of rainfall	1.00	0.64	0.11	0.11	0.15	--

* PREC = precipitation, TRANSP = transpiration, ECEP = evaporation from interception , ESOIL = evaporation from the soil surface, PERC = percolation below the rooting zone, ΔSTORE = soil water storage change

Figures

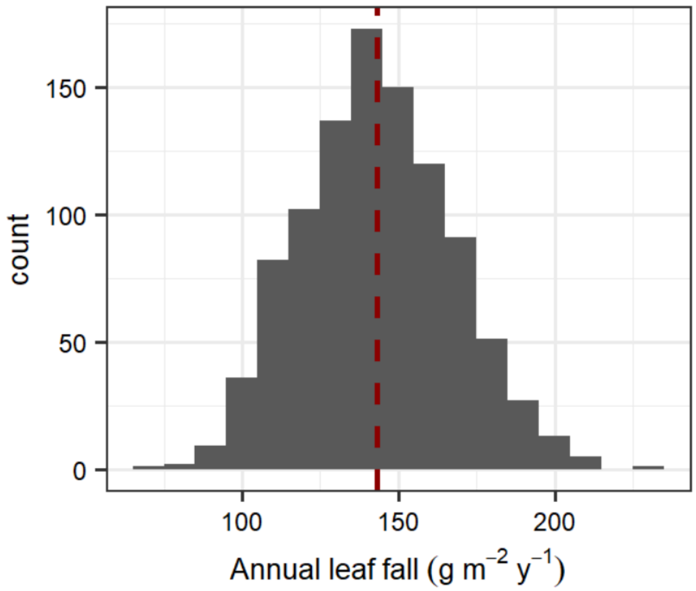

Figure S1: Bootstrapped reconstruction of the cumulated average annual leaf fall (g m^{-2} y^{-1}) in Yatir for the 2003 - 2012 period from leaf trap collection observations. Vertical dashed line indicates the median value, which is the value that has been considered in the main text of the document to compute the total leaf biomass in Yatir.

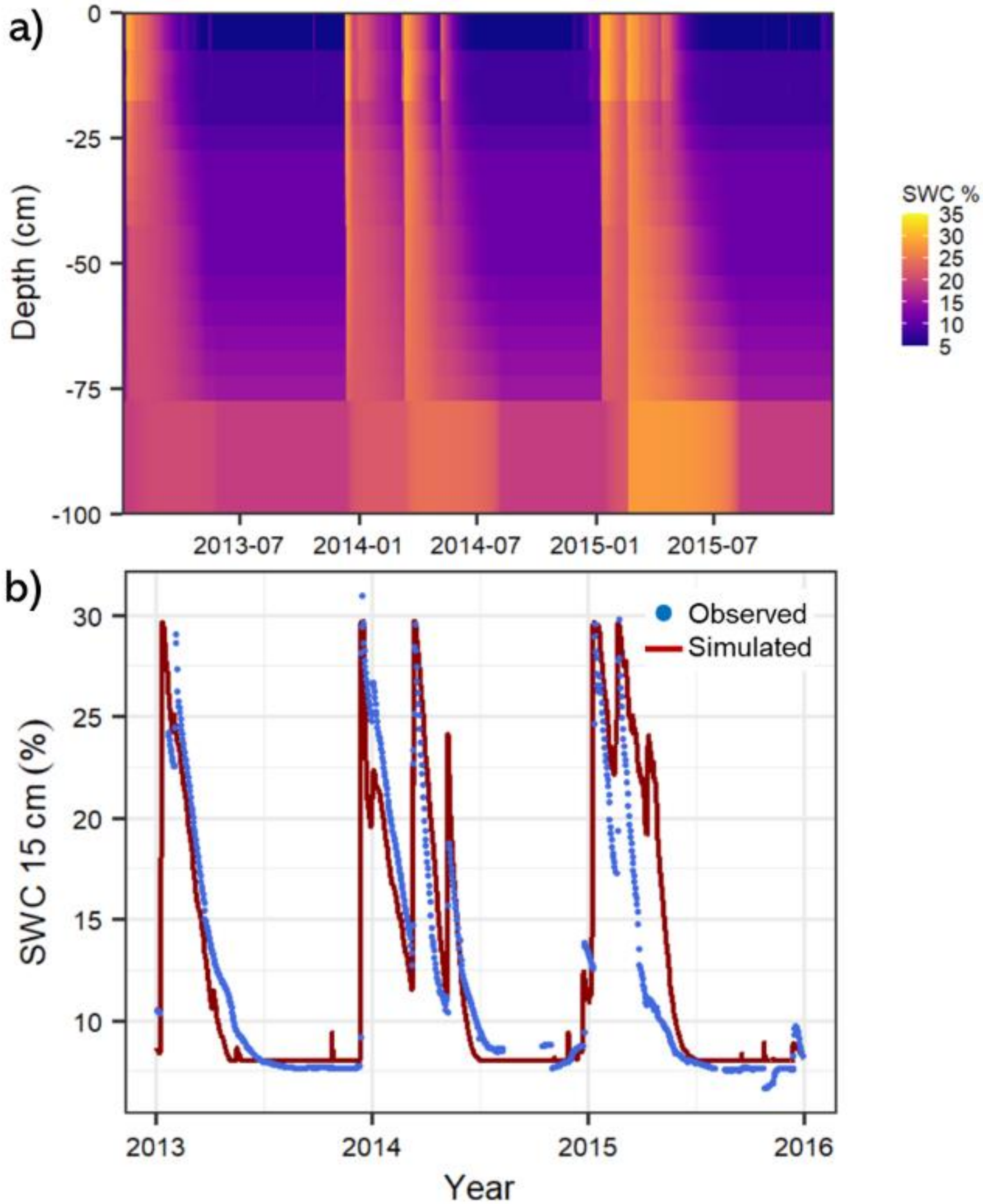

Figure S2: Daily simulated soil water content dynamics in Yatir with calibrated LandscapeDNDC for the 2013 - 2015 period down to 1 m depth, in (a). Comparison of simulated -red line- and measured-blue dots- daily soil water content (SWC, in %) dynamics at the 15 cm soil layer in Yatir for the 2013 - 2015 period, in (b).

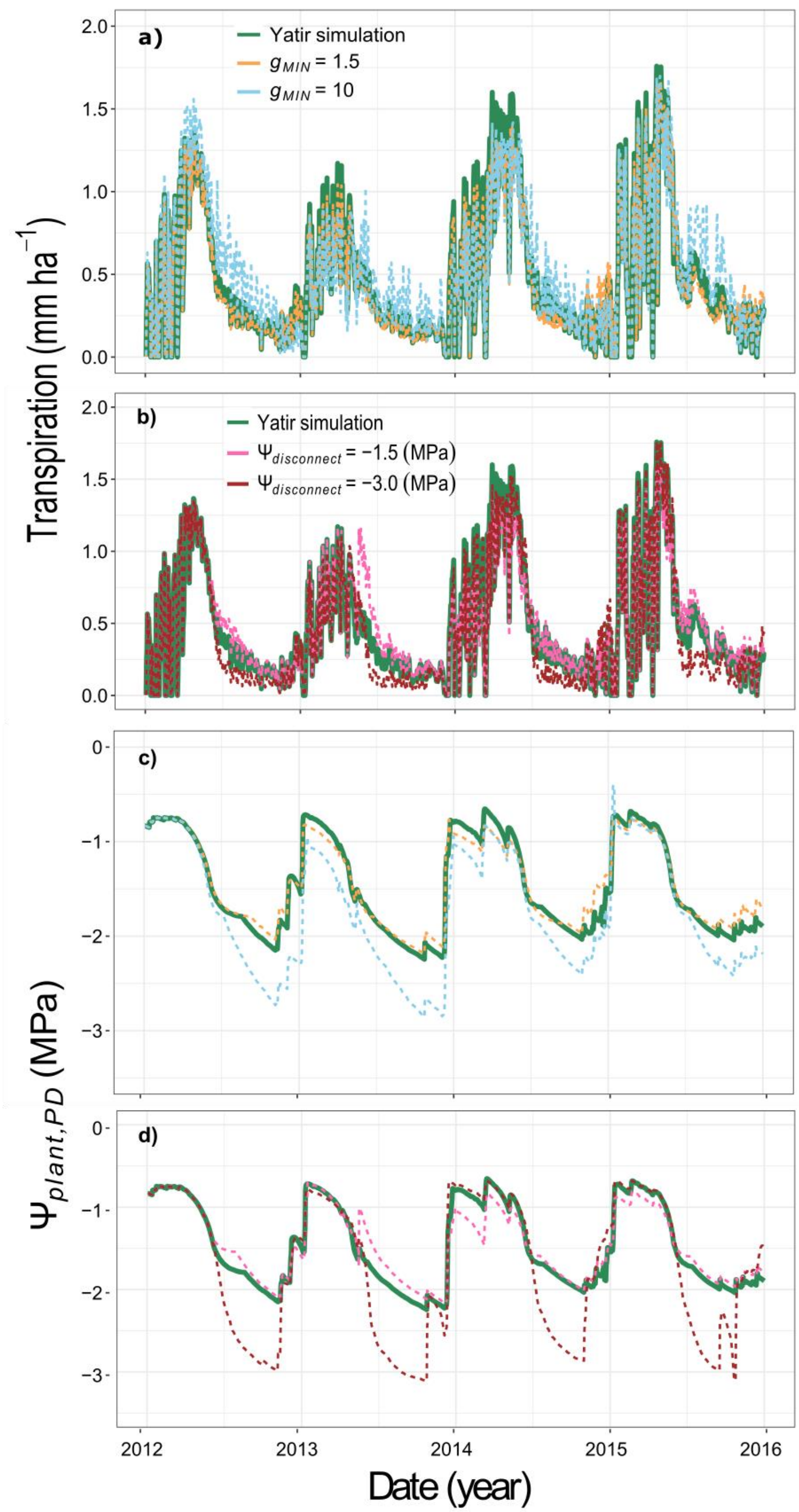

Figure S3: Sensitivity of transpiration (a/b) and plant water potential (c/d) to the parameters g_{MIN} (a/c, Yatir simulation is 3.0 as presented in Table 1)) and $\Psi_{\text{disconnect}}$ (b/d, Yatir simulation is -1.75 as presented in Table 1) throughout the simulation period (2012-2015) at the Yatir forest site.

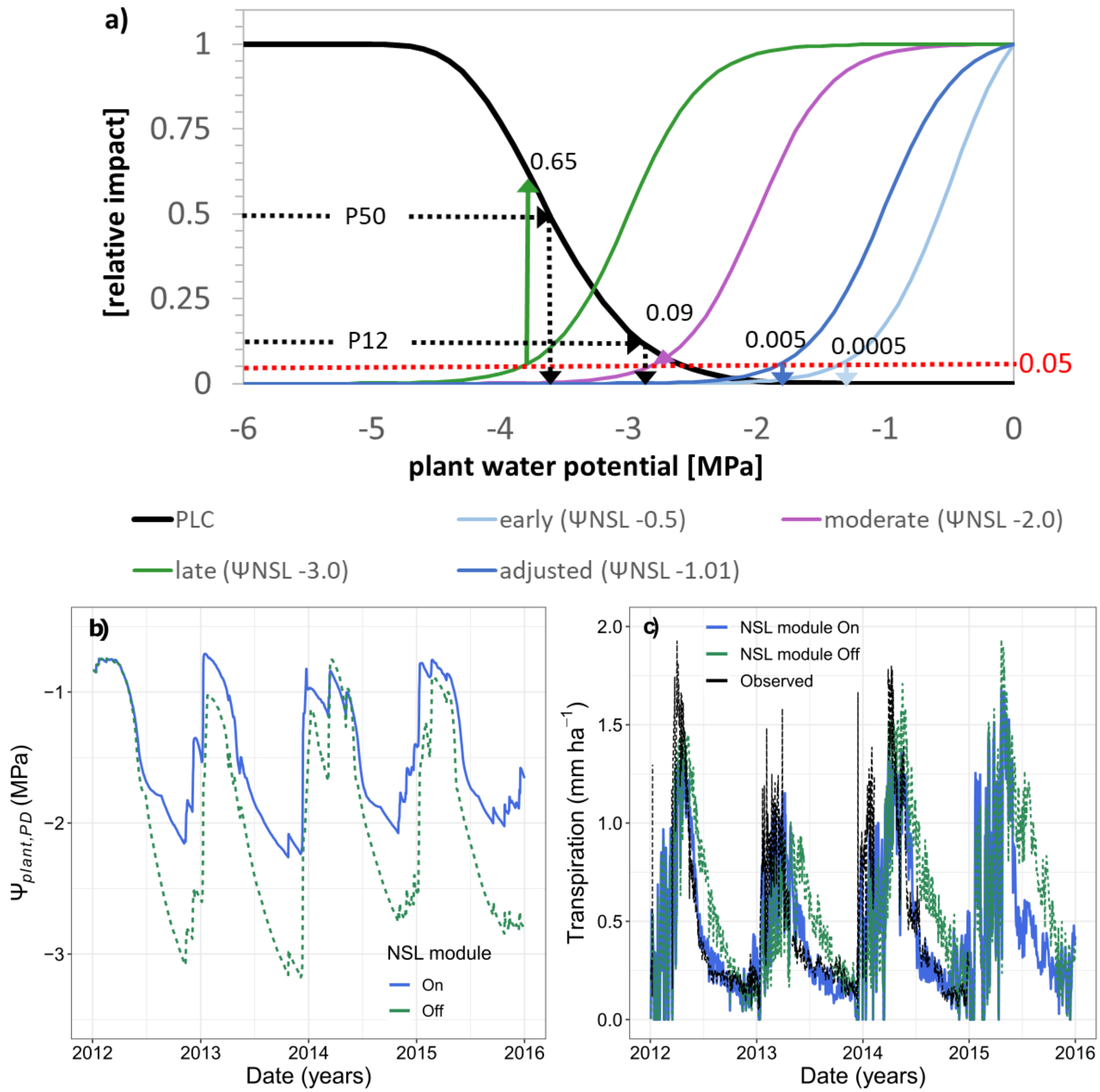

Figure S4: Sensitivity of water balance simulations to the direct photosynthesis effect. a) NSL response curves with different sensitivities to plant water potential (early, moderate, late) and their relation to the percentage loss of conductance (PLC, black line) according to Wagner et al. (2022). The blue line indicates the adjusted response. As an example, the PLC that is caused by a 95% assimilation reduction (red broken line) is indicated (black numbers). b) Development of simulated predawn water potentials using the adjusted NSL response (blue line) or using no NSL response (green broken line) during the period 2012-2015. c) same as before but for transpiration but also including sapflux measurements (black line).

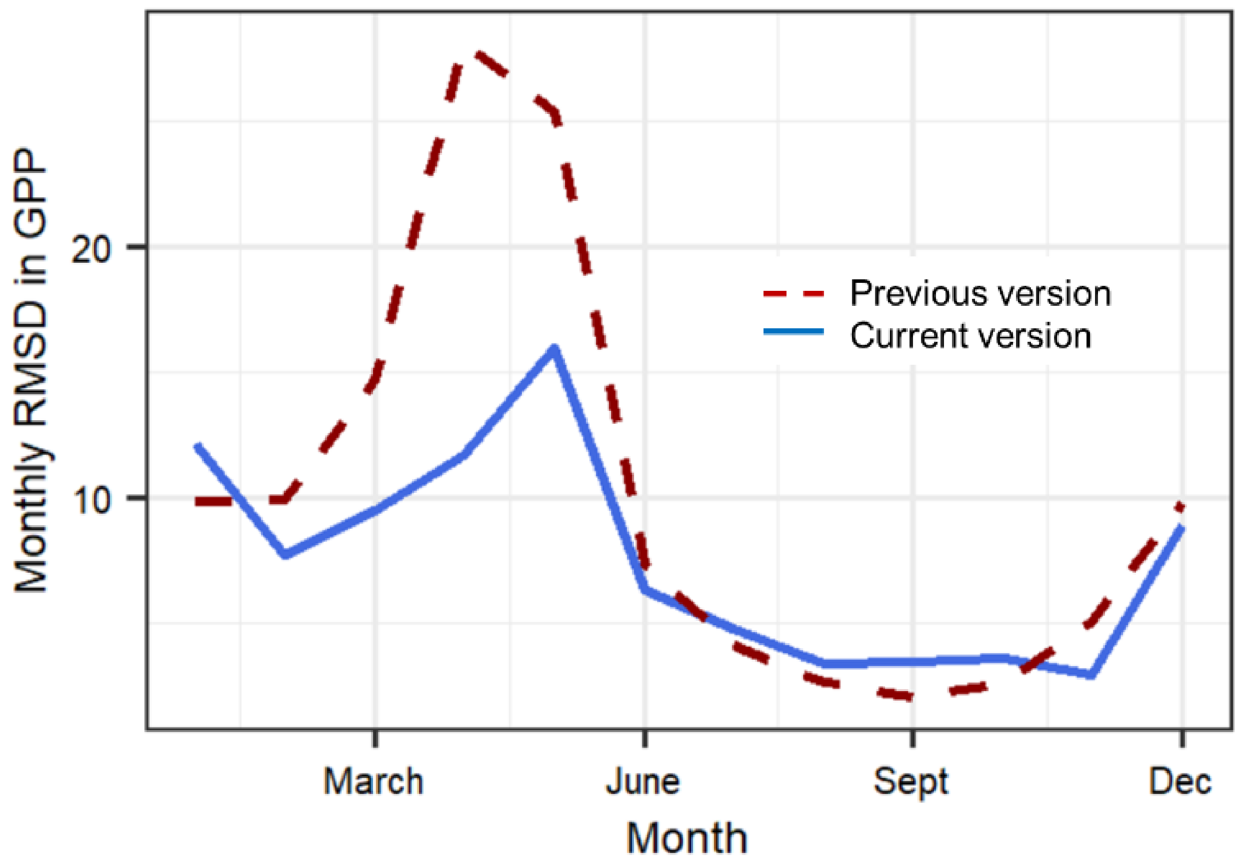

Figure S5: Comparison of the performance in simulating GPP of the current LandscapeDNDC model version including the new hydraulic module with a previous version of the model (Nadal-Sala et al., 2021). The monthly root mean square difference (RMSD) is given for the current (blue line) and the previous (dashed LandscapeDNDC version comparing model output with GPP observations (n = 737) at Yatir from 2013 – 2015. Note the larger the RMSD, the larger the mismatch between model projections and GPP observations.

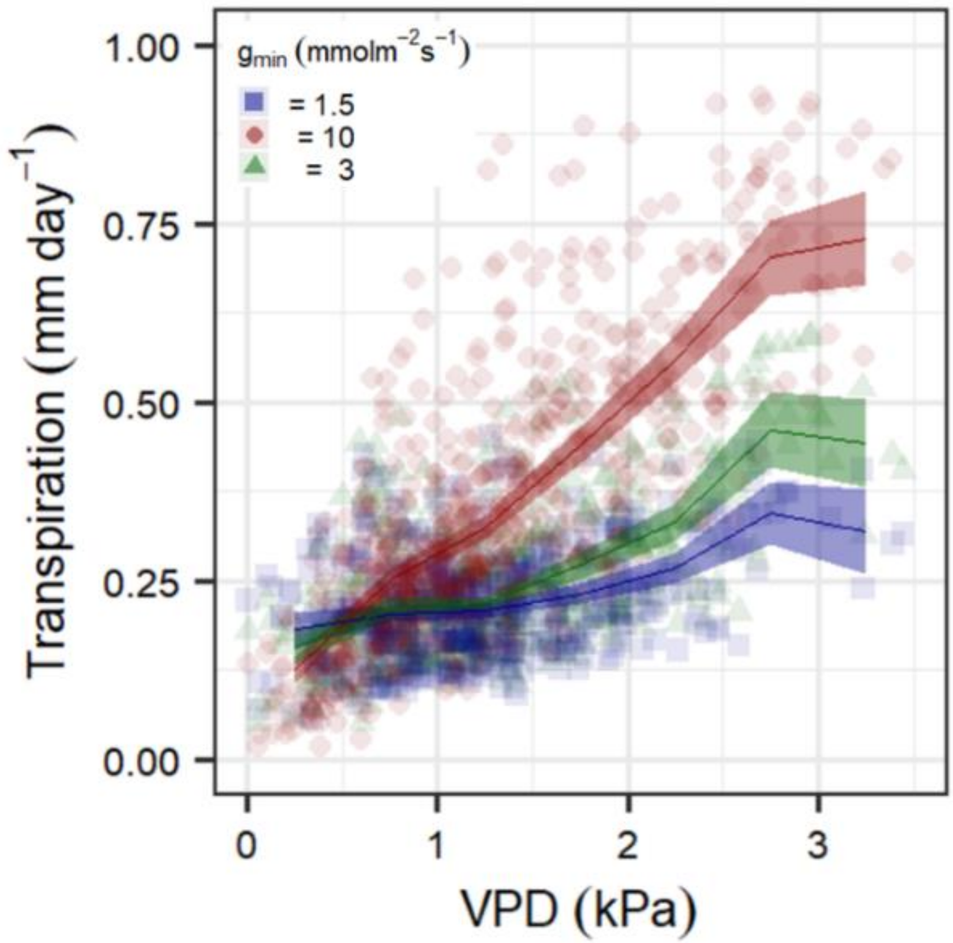

Figure S6: Sensitivity of simulated transpiration to variations in g_{MIN} given for the dry summer period when soil water content was < 11% - corresponding to the point at which roots disconnected from the soil. Given is the daily cumulated transpiration simulated with three different values of g_{MIN} (1.5, 3 and 10 mmol m^{-2} s^{-1}) in relation to changes in daily-averaged vapor pressure deficit in Yatir forest for 2013-2015. Shaded area represents the 0.5 VPD-binned transpiration averages ± 1.96 SE for each g_{MIN}.

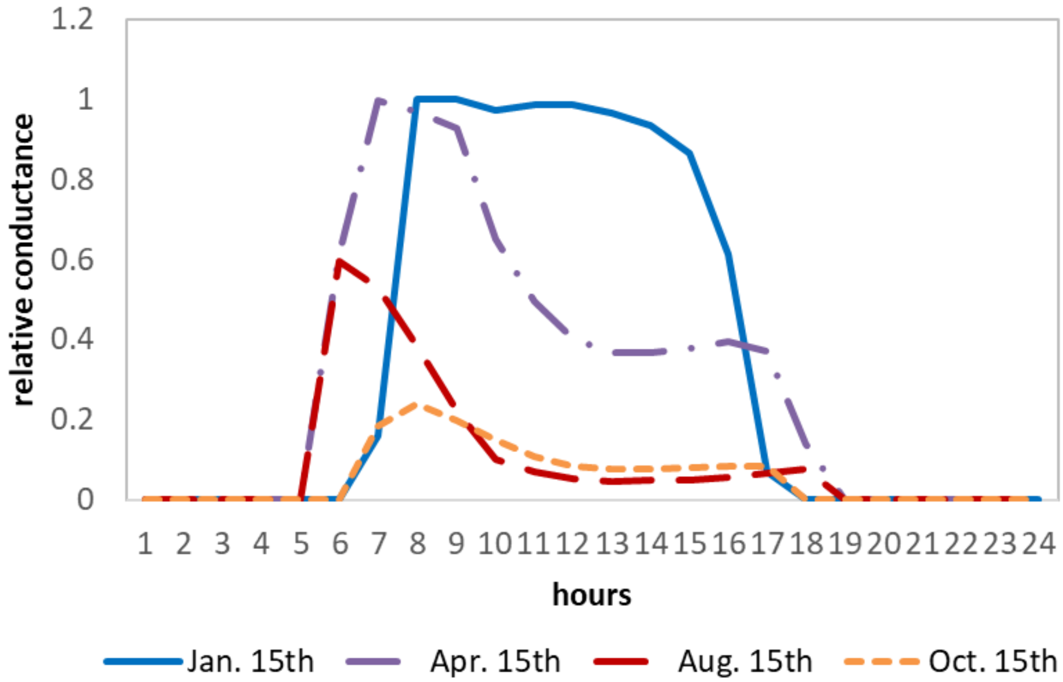

Figure S7: Diurnal course of relative stomatal conductance for different days during the year 2013.

References:

Baquedano, F., and Castillo, F. J.: Drought tolerance in the Mediterranean species *Quercus coccifera*, *Quercus ilex*, *Pinus halepensis* , and *Juniperus phoenicea*, Photosynthetica, 45, 229-238, 10.1007/s11099-007-0037-x, 2007.

Cohen, Y., Cohen, S., Cantuarias-Aviles, T., and Schiller, G.: Variations in the radial gradient of sap velocity in trunks of forest and fruit trees, Plant Soil, 305, 49-59, 10.1007/s11104-007-9351-0, 2008.

Froux, F., Huc, R., Ducrey, M., and Dreyer, E.: Xylem hydraulic efficiency versus vulnerability in seedlings of four contrasting Mediterranean tree species (*Cedrus atlantica, Cupressus sempervirens, Pinus halepensis and Pinus nigra*), Ann. For. Sci., 59, 409-418, 10.1051/forest:2002015, 2002.

Klein, T., and Hoch, G.: Tree carbon allocation dynamics determined using a carbon mass balance approach, New Phytol., 205, 147-159, 10.1111/nph.12993, 2015.

Kuusk, V., Niinemets, Ü., and Valladares, F.: Structural controls on photosynthetic capacity through juvenile-to-adult transition and needle ageing in Mediterranean pines, Funct. Ecol., 32, 1479-1491, 10.1111/1365-2435.13087, 2018.

Maseyk, K., Grünzweig, J. M., Rotenberg, E., and Yakir, D.: Respiration acclimation contributes to high carbon-use efficiency in a seasonally dry pine forest, Glob. Change Biol., 14, 1553-1567, 10.1111/j.1365-2486.2008.01604.x, 2008a.

Maseyk, K. S., Lin, T., Rotenberg, E., Grünzweig, J. M., Schwartz, A., and Yakir, D.: Physiology-phenology interactions in a productive semi-arid pine forest, New Phytol., 178, 603-616, 10.1111/j.1469-8137.2008.02391.x, 2008b.

Nadal-Sala, D., Grote, R., Birami, B., Knüver, T., Schwarz, S., and Ruehr, N.: Leaf shedding and non-stomatal limitations of photosynthesis improve hydraulic resistance of Scots pine saplings during severe drought stress, Front. Plant Sci., 12, 715127, 10.3389/fpls.2021.715127 2021.

Preisler, Y., Tatarinov, F., Grünzweig, J. M., Bert, D., Ogée, J., Wingate, L., Rotenberg, E., Rohatyn, S., Her, N., Moshe, I., Klein, T., and Yakir, D.: Mortality versus survival in drought-affected Aleppo pine forest depends on the extent of rock cover and soil stoniness, Funct. Ecol., 33, 901-912, 10.1111/1365-2435.13302, 2019.

Simioni, G., Marie, G., and Huc, R.: Influence of vegetation spatial structure on growth and water fluxes of a mixed forest: Results from the NOTG 3D model, Ecol. Modelling, 328, 119-135, 10.1016/j.ecolmodel.2016.02.004, 2016.

Sperlich, D., Chang, C. T., Peñuelas, J., Gracia, C., and Sabaté, S.: Seasonal variability of foliar photosynthetic and morphological traits and drought impacts in a Mediterranean mixed forest, Tree Physiol., 35, 501-520, 10.1093/treephys/tpv017, 2015.

Zinsser, J.: Vertical distribution of plant area density and canopy surface temperature of a semi-arid forest, Yatir Israel, Master, Institute of Meteorology and Climate Research - Atmospheric Environmental Research Karlsruhe Institute for Technology, Karlsruhe, 94 pp., 2017.